

# Jahn-Teller like origin of the tetragonal distortion in disordered Fe-Pd magnetic shape memory alloys

Ingo Opahle<sup>1,2</sup>, Klaus Koepernik<sup>1</sup>, Ulrike Nitzsche<sup>1</sup> and Manuel Richter<sup>1</sup>

<sup>1</sup>*IFW Dresden, P.O.B. 270016, D-01171 Dresden, Germany*

<sup>2</sup>*Institut für Theoretische Physik, Universität Frankfurt, 60438 Frankfurt/Main, Germany*

(Dated: March 11, 2022)

The electronic structure and magnetic properties of disordered  $\text{Fe}_x\text{Pd}_{100-x}$  alloys ( $50 < x < 85$ ) are investigated in the framework of density functional theory using the full potential local orbital method (FPLO). Disorder is treated in the coherent potential approximation (CPA). Our calculations explain the experimental magnetization data. The origin of the tetragonal distortion in the Fe-Pd magnetic shape memory alloys is found to be a Jahn-Teller like effect which allows the system to reduce its band energy in a narrow composition range. Prospects for an optimization of the alloys' properties by adding third elements are discussed.

Magnetic shape memory (MSM) alloys have attracted considerable attention as materials for actuator and sensor applications, due to large magnetically induced strains of up to 9.5% in  $\text{Ni}_2\text{MnGa}$ .<sup>1</sup> A promising MSM alloy is disordered  $\text{Fe}_{70}\text{Pd}_{30}$ <sup>2</sup> with a relatively high blocking stress, a high saturation magnetization and a Curie temperature well above room temperature, as well as a high ductility, in contrast to  $\text{Ni}_2\text{MnGa}$ . To date, magnetic field induced strains of about 3% have been observed in Fe-Pd alloys.<sup>3</sup>

The unusually large strains observed in  $\text{Ni}_2\text{MnGa}$  and  $\text{Fe}_{70}\text{Pd}_{30}$ , which are one to two orders of magnitude higher than in conventional magnetostrictive materials, are attributed to a reorientation of martensitic twins in the magnetic field. Twin variants which have their easy axis of magnetization aligned along the field direction gain Zeeman energy and grow at the cost of variants with an unfavorable alignment. This effect thus requires a magnetocrystalline anisotropy energy large enough to prevent a rotation of the magnetization within a twin variant and a high mobility of twin boundaries.

In this Letter, we investigate the electronic structure of disordered  $\text{Fe}_x\text{Pd}_{100-x}$  alloys ( $50 < x < 85$ ) by means of density functional theory calculations. In particular, we explore the electronic origin of the tetragonal distortion resulting in the fct martensite phase, where the MSM effect is observed. On the basis of these results, we discuss prospects for a further optimization of the alloys' properties.

The value of the  $c/a$ -ratio in the fct martensite phase determines the MSM properties of Fe-Pd alloys in a twofold way: First, the maximum strain is given by  $\epsilon = \Delta l/l = |1 - c/a|$  under the assumption of a hundred percent conversion of twin variants. Second, the magnetocrystalline anisotropy energy, which determines the blocking stress, is expected to depend strongly on the  $c/a$ -ratio.<sup>4,5</sup> Thus, understanding the mechanism behind the tetragonal distortion is important for the development of alloys with improved MSM properties.

The martensitic transformation from fcc to fct in disordered Fe-Pd alloys is observed in a narrow composition range between 29 and 32 at% Pd,<sup>6,7</sup> close to the transi-

tion from an fcc to a bcc ground state with increasing Fe content. Upon further cooling an irreversible transition from fct to a (bcc-like) bct phase occurs. The martensite temperature  $T_m$  is close to room temperature for optimal alloy composition, but depends strongly on the Fe content.<sup>6</sup> For applications a martensite temperature  $T_m$  clearly above room temperature would be desirable, since the operation range of MSM elements is limited by  $T_m$ . Attempts to raise  $T_m$  in the Fe-Pd system by addition of Co, Ni, Rh or Pt have so far been unsuccessful.<sup>7,8,9,10</sup> Furthermore, the  $c/a$ -ratio in the martensite phase depends both on composition and on temperature. A gradual increase of  $c/a$  from about 0.92 at  $-80^\circ\text{C}$  to 0.97 near  $T_m$  was observed,<sup>7</sup> similar to the temperature dependence of  $c/a$  in  $\text{Fe}_3\text{Pt}$ , but distinct from the prototype MSM alloy  $\text{Ni}_2\text{MnGa}$ .<sup>3</sup>

We have calculated the electronic structure of disordered  $\text{Fe}_x\text{Pd}_{100-x}$  alloys ( $50 < x < 85$ ) in the framework of density functional theory (DFT) in the local spin density approximation (LSDA) using the high precision full potential local orbital (FPLO, version 5.00-19) method<sup>11</sup> in the scalar relativistic approximation. Disorder was treated within the coherent potential approximation (CPA)<sup>12</sup> and the LSDA parameterization of Perdew and Wang<sup>13</sup> was employed. The basis set consisted of Fe 3spd4sp and Pd 4spd5sp optimized local orbitals. The exponent of the confining potential in the basis optimization was set to  $n = 6$ , which provided lower total energies and a better numerical stability compared to the default value  $n = 4$ . For the  $\mathbf{k}$ -space integrations 1728 points in the full Brillouin zone (FBZ) were used, and the results were cross-checked with 8000 points in the FBZ. Additionally, we have performed calculations with the Akai-KKR code<sup>14</sup> in the muffin tin approximation using the generalized gradient approximation (GGA) to DFT in the parameterization by Perdew *et al.*<sup>15</sup>

The calculated magnetic moments of fcc  $\text{Fe}_x\text{Pd}_{100-x}$  alloys ( $50 < x < 70$ ) are in an overall good agreement with the experimental data by Matsui *et al.*<sup>16</sup> The average spin moment per atom, calculated with FPLO at the respective experimental lattice parameter, increases approximately linearly with increasing Fe content from 1.55

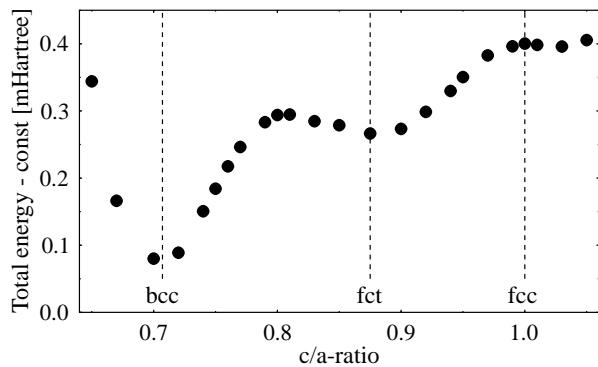


FIG. 1: Total energy as a function of  $c/a$ -ratio for  $\text{Fe}_{80}\text{Pd}_{20}$  calculated with the atomic volume fixed to  $V_{\text{at}}=13.256 \text{ \AA}^3$ . The total energy exhibits a local minimum at  $c/a=0.875$  corresponding to an fct martensite structure.

$\mu_B$  for  $x = 50$  to  $1.98 \mu_B$  for  $x = 70$ . Adding the contributions of the orbital moments, which are estimated from relativistic supercell calculations<sup>5</sup> to be about  $0.13 \mu_B$  for Fe and  $0.04 \mu_B$  for Pd, the calculated moments agree within  $0.05 \mu_B$  with the experimental values for the average total moments  $1.61 \mu_B$  ( $x = 50$ ) and  $2.04 \mu_B$  ( $x = 70$ ).

Assuming that the individual atomic moments do not depend on the composition, Matsui *et al.*<sup>16</sup> had to use an unusually large Pd moment of  $0.56 \mu_B$  to fit the concentration dependence of their magnetization data. This value is nearly twice the value we obtained for the Pd spin moment ( $0.29 \mu_B$ ). Our calculations provide a different explanation for the observed concentration dependence. The spin moment of Fe decreases with increasing Fe content due to magneto volume effects, from about  $2.82 \mu_B$  for  $x = 50$  to  $2.71 \mu_B$  for  $x = 70$ . A yet more pronounced reduction of the Fe moments with increasing Fe content was recently observed in neutron scattering experiments on  $\text{L1}_0$ -ordered FePt alloys<sup>17</sup>.

The fcc structure can be continuously transformed into a bcc structure by a change of the  $c/a$ -ratio, the so called Bain path. A (meta) stable fct phase must exhibit a (local) minimum in the free energy along the Bain path for  $0.71 < c/a < 1$ . In our total energy calculations we find such a local minimum only in a narrow region of phase space, where the total energy differences between fcc and bcc are small and the energy landscape along the Bain path is accordingly flat (Fig. 1). This is in agreement with the experimentally observed proximity of the martensite phase to the transition from an fcc to a bcc ground state. While in the LSDA calculations the fcc-bcc transition is found at a somewhat higher Fe concentration  $x \approx 80$  in the vicinity of the experimental volume, the KKR GGA data yield almost exactly the experimental value  $x \approx 70$ .

Further insight into the origin of the martensite phase is obtained from the density of states (DOS) shown in Fig. 2. The DOS in the vicinity of the Fermi energy is

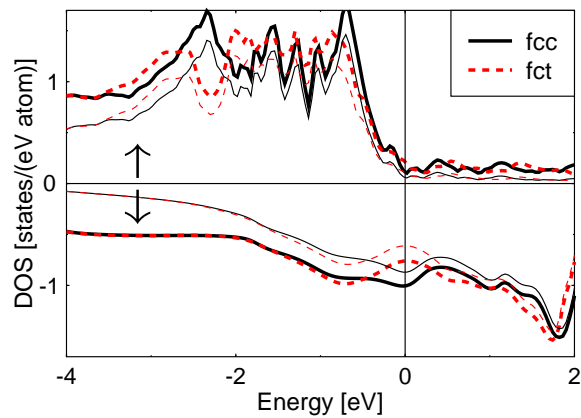


FIG. 2: (Color online) DOS of  $\text{Fe}_{80}\text{Pd}_{20}$  in the fcc (solid lines) and fct (dashed lines) structures corresponding to Fig. 1. The total DOS (thick lines) and the partial Fe 3d DOS (thin lines) are shown. The minority spin DOS ( $\downarrow$ ) exhibits a peak at the Fermi energy (vertical line) in fcc which splits in fct.

dominated by Fe 3d states, which are hybridized with Pd 4d states (not shown). The majority spin channel of the Fe 3d subshell is completely filled, while in the partially filled minority spin channel a peak is located right at the Fermi energy in the fcc austenite phase. In the fct martensite phase this peak is split and weight is shifted below and above the Fermi energy, indicative of a cooperative Jahn-Teller effect. The gain in band energy due to this splitting (estimated from a single step calculation) is a few tenths of a mHartree.

Further support for a Jahn-Teller like origin of the tetragonal distortion in the disordered Fe-Pd MSM alloys is obtained from the spectral density of the minority spin states shown in Fig. 3. For the cubic austenite phase (upper panel) the threefold degenerate  $t_{2g}$  states of the Fe 3d minority spin shell are located right at the Fermi level close to the  $\Gamma$ -point (note that due to disorder a broadening of the bands occurs). The tetragonal distortion in the martensite phase (lower panel) causes a splitting of the  $t_{2g}$  states, which are shifted away from the Fermi energy, resulting in a gain in band energy in a Jahn-Teller like fashion.

On the basis of the results discussed above, the following conclusions can be drawn: The presence of degenerate Fe 3d minority spin bands at the Fermi energy in Fe-Pd MSM alloys favors a structural distortion, which is stabilized by a gain in band energy. However, due to band dispersion and disorder, this energy gain is small and thus can only compete with other energy terms (like the Madelung energy favoring close packed structures) if the energy landscape is sufficiently flat, i.e. close to the fcc-bcc transition. The gain in band energy due to the Jahn-Teller like splitting is approximately proportional to the height of the peak in the minority spin DOS. The energy difference between fcc and bcc changes by approximately  $4 \text{ meV/at\%}$ , while the height of the peak in the DOS shows only a moderate concentration dependence.

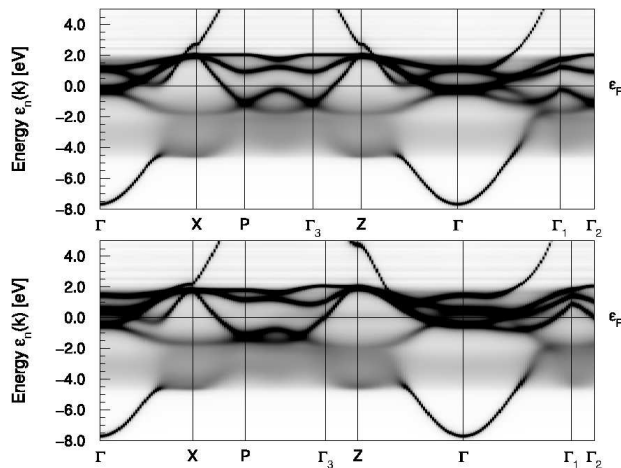


FIG. 3: CPA minority spin spectral densities of  $\text{Fe}_{80}\text{Pd}_{20}$  in the fcc structure (upper panel) and fct (lower panel) corresponding to Fig. 1.

Thus already small deviations from the optimal stoichiometry result in relatively steep energy curves along the Bain path and cause the local fct minimum to disappear. Consequently, a stabilization of the fct structure in terms of  $c/a$ -ratio and martensite temperature  $T_m$  is expected with increasing iron concentration  $x$ , up to the point where a bcc (or bct) structure becomes favorable. Alternatively, alloying Fe-Pd with ternary elements could lead to a stabilization of the fct phase. According to our KKR GGA calculations, Fe-Pd-X alloys with about 5 at% of the ternary elements  $X = \text{W}, \text{Au}$  or  $\text{Pt}$  show a more pronounced peak in the minority spin DOS close to the respective fcc-bcc transition and are therefore interesting candidates for MSM alloys with enhanced  $T_m$ .

Our results imply that  $T_m$  and  $c/a$  in Fe-Pd(-X) alloys are determined by a delicate balance between the energy gain due to the Jahn-Teller splitting and the proximity to the fcc-bcc transition. This is in line with the experimentally observed  $T_m$  of binary and ternary Fe-Pd(-X) MSM alloys ( $X = \text{Co}, \text{Ni}, \text{Pt}$ ), which shows a strong increase with the Fe concentration  $x$  for alloys having a comparable amount of the ternary element  $X$  (Fig. 4). The critical Fe concentration  $x_c$ , where fcc and bcc are de-

generate in energy depends on the amount and the type of  $X$  (Fig. 4). The values of  $x_c$  have been obtained from KKR GGA calculations and depend below 10 at% of  $X$  approximately linear on the amount of ternary element. The KKR GGA calculations yield  $x_c$  for the binary alloys in excellent agreement with the experimental trends, and the relative trends upon alloying can be considered trustworthy despite the limited accuracy of the muffin tin approximation. For Co and Ni,  $x_c$  is shifted to lower values, while for Pt it is increased with respect to the binary system. This naturally explains that in the experiments of Ref. 10 addition of Pt at constant Fe content was found to have a negative influence on  $T_m$ , as with increasing Pt content  $x_c$  was shifted away from 70 at% Fe concentra-

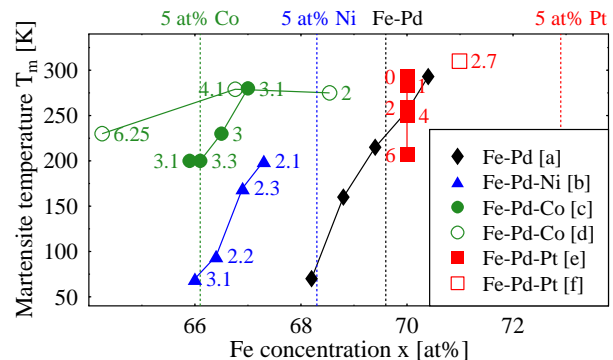


FIG. 4: Experimental martensite temperature as a function of the Fe concentration  $x$  for  $\text{Fe}_x\text{Pd}_{100-x}$  (a: Ref. 6),  $\text{Fe}_x\text{Pd}_{100-x-y}\text{Ni}_y$  (b: Ref. 8),  $\text{Fe}_x\text{Pd}_{100-x-y}\text{Co}_y$  (c: Ref. 8; d: Ref. 9), and  $\text{Fe}_x\text{Pd}_{100-x-y}\text{Pt}_y$  (e: Ref. 10, f: Ref. 9). Numbers near data points indicate the amount of ternary element  $y$ . Also shown is the calculated Fe concentration  $x_c$  for the fcc-bcc transition (dashed vertical lines) for Fe-Pd and ternary alloys with  $y = 5$  at%.

tion used. The somewhat higher value of  $T_m$  observed in Ref. 9 is in line with our argument. Consequently, a careful optimization of the Fe content is necessary to achieve  $T_m$  enhancement in ternary Fe-Pd-X alloys.

This work was supported financially by the DFG, SPP 1239. Discussions with Monodeep Chakraborty are gratefully acknowledged.

<sup>1</sup> A. Sozinov *et al.*, Appl. Phys. Lett. **80**, 1746 (2002).

<sup>2</sup> R. D. James, M. Wuttig, Phil. Mag. A **77**, 1273 (1998).

<sup>3</sup> T. Kakeshita, T. Fukuda and T. Takeuchi, Mat. Sci. Eng. A **438-440**, 12 (2006).

<sup>4</sup> J. Lyubina *et al.*, J. Phys.: Condens. Matter **17**, 4157 (2005).

<sup>5</sup> J. Buschbeck *et al.*, Phys. Rev. B **77**, 174421 (2008).

<sup>6</sup> M. Sugiyama, R. Oshima and F. E. Fujita, Mater. Transact. JIM **25**, 585 (1984).

<sup>7</sup> R. Oshima and M. Sugiyama, J. Phys. (Paris) **43**, 383 (1982).

<sup>8</sup> K. Tsuchiya *et al.*, Mater. Trans. **44**, 2499 (2003).

<sup>9</sup> D. Vokoun *et al.*, Smart Mater. Struct. **14**, S261 (2005).

<sup>10</sup> T. Wada, T. Tagawa, M. Taya, Scripta Mater. **48**, 207 (2003).

<sup>11</sup> K. Koepf and H. Eschrig, Phys. Rev. B **59** 1743 (1999); <http://www.FPLO.de>.

<sup>12</sup> K. Koepf *et al.*, Phys. Rev. B **55**, 5717 (1997).

<sup>13</sup> J.P. Perdew and Y. Wang, Phys. Rev. B **45**, 13244 (1992).

<sup>14</sup> <http://sham.phys.sci.osaka-u.ac.jp/~kkf/>.

<sup>15</sup> J. P. Perdew *et al.*, Phys. Rev. B **46**, 6671 (1992).

<sup>16</sup> M. Matsui and K. Adachi, Physica B **161**, 53 (1989).

<sup>17</sup> J. Lyubina *et al.*, Appl. Phys. Lett. **89**, 032506 (2006).